Available online at www.sciencedirect.com

ScienceDirect

Energy Procedia 71 (2015) 149 – 158

Energy Procedia

The Fourth International Symposium on Innovative Nuclear Energy Systems, INES-4

Preliminary Safety Analysis of Mixed Oxide Sphere-pac Driver Fuels in the CP-ESFR WH Core

Lena Andriolo[a,*], Xue-Nong Chen[a], Claudia Matzerath Boccaccini[a], Andrei Rineiski[a], Werner Maschek[a], Fabienne Delage[b], Elsa Merle-Lucotte[c]

[a]Institute for Nuclear and Energy Technologies (IKET), Karlsruhe Institute of Technology (KIT)
Hermann-von-Helmholtz-Platz 1, D-76344 Eggenstein-Leopoldshafen, Germany
[b]Département d'Etudes des Combustibles (DEC), Commissariat à l'Energie Atomique et aux Energies Alternatives de Cadarache (CEA-Cadarache), F-13108 Saint-Paul-lès-Durance, France
[c]Laboratoire de Physique Subatomique et de Cosmologie (LPSC), Centre National de la Recherche Scientifique (CNRS), 53 rue des Martyrs, F-38026 Grenoble, France

Abstract

Future sodium cooled fast reactors (SFRs) with Minor Actinide (MA) burning potential have to demonstrate an enhanced safety, minimal waste production and increased proliferation resistance in addition to their high economical potential. In this context, the PELGRIMM project, part of the European Framework Program 7 (FP7), investigates new MA-bearing oxide fuel developments for SFRs. Two fuel designs are studied: the standard pellet and the innovative sphere-pac fuel. Due to its favorable swelling behavior expected under irradiation and its dustless fabrication, the latter one appears to be a promising option. A special work package in PELGRIMM addresses the safety performance of this fuel under operational, design basis (DBC) and design extension conditions (DEC). For the preliminary safety assessment, the Working Horse (WH) core, designed and analyzed in the former CP-ESFR project was chosen. The SIMMER-III code was applied after implementing key features as the specific thermal conductivity of sphere-pac fuels. The feasibility of loading the core with MOX sphere-pac instead of pellet fuel, regarding operation and safety limitations, was first proven. Both fuel designs for the WH core at beginning of life and after irradiation were then compared at nominal and under unprotected loss of flow conditions. Results show a similar behavior of these fuels under irradiation, opening a perspective to the practical application of sphere-pac fuels in SFR systems.

Selection and peer-review under responsibility of the Tokyo Institute of Technology

Keywords: Sphere-pac fuel; Severe accidents; SIMMER-III; PELGRIMM; Sodium fast reactor safety

* Corresponding author. Tel.: +49-721-6082-2478; fax: +49-721-6082-3824.
E-mail address: lena.andriolo@kit.edu

Selection and peer-review under responsibility of the Tokyo Institute of Technology
doi:10.1016/j.egypro.2014.11.865

1. Introduction

In the framework of the Generation IV International Forum, six nuclear energy systems employing various fuel cycles, energy conversion and reactor technologies are currently under study. All systems have to prove their high safety level, competitiveness, proliferation resistance and sustainability - in terms of improved fuel utilization, breeding capacity and waste management.

Nomenclature

Symbols or letters

α	volume fraction	(-)
k	thermal conductivity	($W.m^{-1}.K^{-1}$)
h	heat transfer coefficient	($W.m^{-2}.K^{-1}$)
$\bar{\rho}$	macroscopic density	($kg.m^{-3}$)
e	specific energy	($J.kg^{-1}$)
a	area per unit volume	(m^{-1})
Q	energy transfer rate per unit volume	($W.m^{-3}$)
p	pressure	(Pa)
t	time	(s)

Subscripts

i	initial
int	fuel interior
s1	fuel surface
s4	cladding
nf, pin	non flow, pin
m	temperature node
H	fluid
N	nuclear heating

Accordingly, different fuels for transmutation demonstrating higher safety potential are under investigation, one of them being the sphere-pac concept. In this concept, fuel microspheres are poured into a cladding tube and compacted by vibration. These fuels seem to be good candidates to MA-bearing fuel concepts due to their dustless production and their good swelling behavior under irradiation. Nevertheless, their safety behavior under severe accident conditions, especially at beginning of life (BOL), raises some concerns.

The objective of the subsequent study performed in the frame of the FP7-PELGRIMM project [1] is to propose a comparative evaluation of the CP-ESFR WH core [2] loaded with either sphere-pac or pellet driver fuel in reference to safety performances both under nominal and accidental conditions. In this paper focus is on the basic feasibility of implementing innovative sphere-pac fuels into a core originally filled with pellet fuel and on the behavior of this core during Hypothetical Core Disruptive Accidents (HCDAs) in particular after an unprotected loss of flow (ULOF). The WH core was chosen for its extended safety analyses performed in the CP-ESFR project [3]. Within the PELGRIMM project an optimized ESFR, the CONF-2 design, will be investigated in the next step [4].

The study is performed with SIMMER-III [5]: a two-dimensional, multi-velocity-field, multiphase, multicomponent, Eulerian fluid-dynamics code coupled with a space/time-dependent neutron kinetics model and a fuel pin model.

In the following, main characteristics of sphere-pac fuels, models and assumptions used to perform the calculations are described. A preliminary safety analysis and comparison of the WH loaded with either sphere-pac or pellet fuels is then detailed for BOL and end of equilibrium cycle (EOEC) conditions.

2. Sphere-pac fuels

Sphere-pac fuels are investigated worldwide since the 1960s. These fuels are expected to present several advantages when it comes to the use of minor actinides in nuclear fuels. As sphere-pac pins are composed by fuel microspheres of several particle size ranges poured into a cladding tube and surrounded by Helium gas, they are expected to behave well under irradiation. In fact, their specific macrostructure would provide enough space for fission gases and He released by MA decay to be accommodated and to relieve pressure on the cladding [6]. Sphere-pac fuels are fabricated by sol-gel methods. This "wet" route limits the contamination risk of operators and facilities as it is a dustless process. Grinding and milling steps required in the standard pellet fabrication are hence avoided. One major drawback of sphere-pac fuel stacks (compared to pellets) is their lower thermal conductivity at BOL. Indeed, due to the few and narrow contact points between the spheres, the heat transfer is reduced. This drawback is compensated during the early lifetime of sphere-pac fuels as they rapidly restructure in the core - on a timescale of hours - due to the strong temperature gradients in the fuel - Fig. 1. The thermal conductivity of sphere-pac fuels is therefore already enhanced during the start-up phase, due to sintering mechanisms as demonstrated, e.g., in the FUJI experiment [6].

3. Thermal conductivity and heat transfer modeling in SIMMER-III

3.1. Thermal conductivity of sphere-pac and pellet fuels

A first step toward the feasibility and safety performance assessment of sphere-pac fuels is to quantify the heat transfer in these pins. A key parameter here is the maximum achievable packing fraction of spheres and the related porosity as they finally define the fuel thermal conductivity. It was demonstrated in [7] that smear densities as high as 95% of the theoretical density (TD) could be reached by packing spheres of different sizes. Hence, using sphere-pac fuels instead of pellet fuels doesn't impact core neutronics as the fuel mass is kept equal.

In SIMMER-III the conductivity of solid fuel is expressed as a function of temperature and corrected by the Maxwell-Eucken formula to take into account the effect of porosity [8]. In the subsequent part, emphasis is put on assessing the thermal conductivity of both fuel types at different irradiation states.

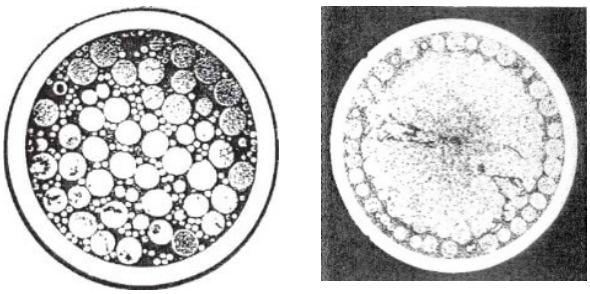

(a) (b)

Fig. 1. (a) non irradiated sphere-pac pin; (b) irradiated sphere-pac pin [6].

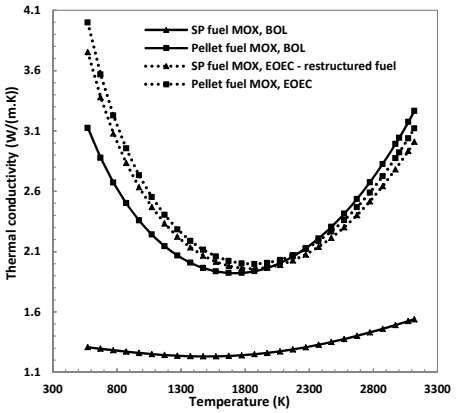

Fig. 2. Thermal conductivity of sphere-pac (SP) and pellet fuel in the WH at BOL and EOEC.

- Beginning of life

The WH core contains pellet fuel with 5.00% porosity and a smear density of 83.41%TD. In case of sphere-pac fuels this implies that the microspheres' porosity and the Helium surrounding them add up to a volume faction of 16.59%. In order to evaluate the thermal conductivity of non-restructured sphere-pac fuels an extensive literature study was fulfilled and the equation primarily elaborated upon Hall and Martin was chosen [9]. The result is displayed in Fig. 2. It can be noticed, that the thermal conductivity of BOL sphere-pac fuels used in the WH is significantly lower than the one of pellet fuels.

- End of equilibrium cycle

After 3 irradiation cycles, when the fuel represents the average fuel in the core at EOEC, the WH pellet fuel is assumed to have a porosity of 7.50% and an oxygen over metal ratio of 2 [10]. At this stage of irradiation, a pin filled with sphere-pac fuel exhibits, in first approximation, two zones: one outer non-restructured zone displaying the BOL structure, and one restructured zone with properties similar to a pellet fuel of same density. Characteristics of EOEC fuels are listed in Table 1.

To assess the thermal conductivity of restructured sphere-pac fuel, conductivity correlations in each of the two zones are determined and both conductivities are then combined into one single equation based on the linear power of each zone. This gives the effective fuel thermal conductivity. In the non-restructured zone, Hall and Martin's approach is used while in the restructured zone Philiponneau's equation for MOX fuels is applied [11].The thermal conductivity of pellet fuels is also obtained with [11]. A summary of conductivities for both fuels at BOL and EOEC is pictured Fig. 2.

Table 1. Sphere-pac and pellet fuel characteristics at EOEC in the WH

	Standard MOX pellet pin	Restructured MOX sphere-pac pin
Fuel smear porosity (*%*)	16.59	16.59
Fuel porosity and other characteristics	Fuel porosity 7.5%	2 fuel zones: restructured and non-restructured
		2 sphere diameters: 1200μm or 35 μm
		Restructured zone porosity 7.5%
Central hole diameter (*mm*)	3.05	2.92 (30% of cladding inner diameter)
Burn up (*%at*)	6	6
Oxygen over metal ratio	2	2
Gap state	Closed gap	No gap

3.2. Fuel pin heat transfer modeling in SIMMER-III

SIMMER-III was primarily developed to evaluate the behavior of an already disrupted reactor core where most pins already failed. Therefore a simplified fuel-pin model (SPIN) was originally implemented [12]. A detailed pin model (DPIN) was later added to simulate more accurately the radial heat transfer in the fuel as well as potential molten cavity generation and in-pin fuel motion of still existing pin structures [12]. Focusing on the ULOF (with clad failure preceding fuel failure) and given the lack of transient experiments with sphere-pac fuels, the SPIN model was chosen for simulation. It describes the fuel pellet and cladding with 2 and 1 nodes, respectively, see Fig. 3. The 2 pellet nodes referred to as interior and surface node describe the fuel bulk and surface temperatures, respectively.

The fuel surface node thickness is defined with the thermal penetration length $2\delta_f$, while considering the transient thermal response of the surface node. The node dimensions are recalculated at each heat transfer time step. Heat transfer coefficients between the two fuel nodes (Eq.1) and from the surface node to the cladding (Eq.2) are determined as follows:

$$h_{int,S1} = \frac{1}{r_{p1}}\left(\frac{1}{k_{int}} ln\left(\frac{r_{p1}}{r_{p0}}\right) + \frac{1}{k_{S1}} ln\left(\frac{r_{p2}}{r_{p1}}\right)\right)^{-1} \quad (1)$$

$$h_{S1,S4} = \left(\frac{r_{p3}}{k_{S1}} ln\left(\frac{r_{p3}}{r_{p2}}\right) + \frac{1}{h_{gap}} + \frac{r_{p4}}{k_{S4}} ln\left(\frac{r_{p5}}{r_{p4}}\right)\right)^{-1} \quad (2)$$

The fuel pin heat transfer rate is then calculated, Eq. 3:

$$\frac{\partial \overline{\rho_m} e_m}{\partial t} = h_{m,m-1} a_{m,m-1} (T_{m-1} - T_m) + h_{m+1,m} a_{m+1,m} (T_{m+1} - T_m) + Q_{Hm} + Q_{Nm} \quad (3)$$

In the above mentioned procedure, the gap conductance used to determine h_{gap} is recalculated during each time step. The fuel pin failure is based on a thermal criterion depending on melting fractions of fuel and cladding. Pin breakup modeling includes the downfall or collapse of unsupported pellets.

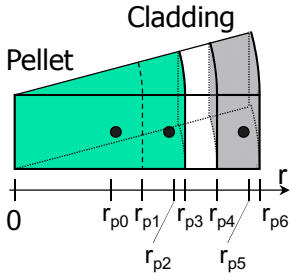

$$r_{pin} = r_{p6} = r_{pin}^{i} \sqrt{\frac{\alpha_{pin}}{\alpha_{pin}^{i}}}$$

$$r_{p4} = r_{pin} \sqrt{\frac{\alpha_{int} + \alpha_{s1} + \alpha_{nf,PIN} + \alpha_{s4}}{\alpha_{pin}}}$$

$$r_{p3} = r_{pin} \sqrt{\frac{\alpha_{int} + \alpha_{s1}}{\alpha_{pin}}}$$

$$r_{p1} = r_{p3} - 2\delta_f$$

$$r_{p5} = \sqrt{\frac{r_{p4}^2 + r_{p6}^2}{2}}$$

$$r_{p2} = \sqrt{\frac{r_{p1}^2 + r_{p3}^2}{2}}$$

$$r_{p0} = \frac{r_{p1}}{\sqrt{2}}$$

Fig. 3. Radii calculation for SIMMER-III pin modeling. [9]

4. SIMMER-III calculations, results and discussion

4.1. Steady state calculation

- Modeling

  The WH was modeled in SIMMER-III in R-Z geometry i.e. the core was transformed into concentric rings. One

should note that the WH radial power distribution is extremely non-uniform at BOL with a high peak in the second core zone [2,10], as the power profile was optimized for EOEC. Axially, the sodium below the core, the assemblies' lower and upper part, the lower and upper gas plenum, the steel blanket and reflectors, and the sodium plenum are modeled, see Fig.4. The total pressure drop in the core is 4.5 bar. Assemblies' inlet orifices are chosen to reach similar coolant temperatures at core outlet. A stationary state is obtained with SIMMER-III after 50s and near design pressure and temperature distributions are achieved.

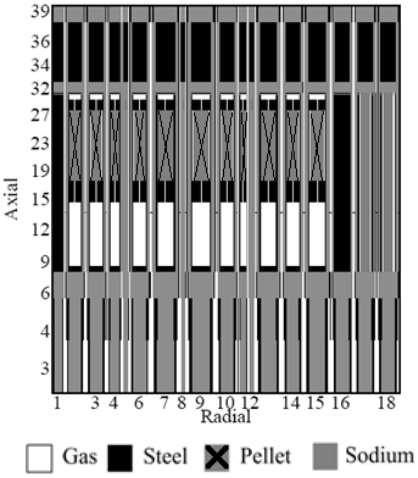

Fig. 4. WH modeling in SIMMER-III.

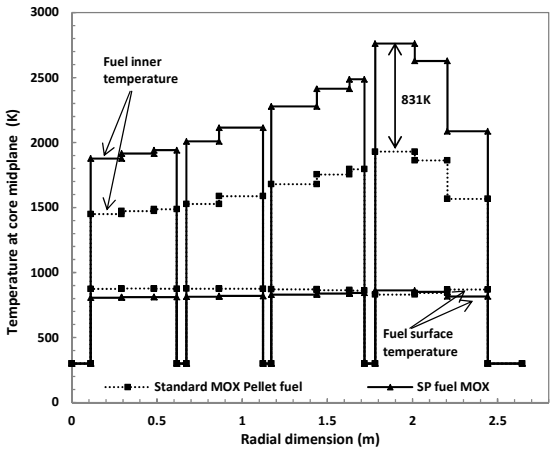

Fig. 5. BOL radial temperature distributions in the WH loaded with either sphere-pac (SP) or pellet fuel.

- BOL calculations

One essential difference between pellet and sphere-pac pins used in the WH is that the pellets are annular whereas the sphere-pac pins do not contain a central hole at BOL. Thus, the sphere-pac pins' central temperature is higher than the pellet one even though no gap between fuel and clad exists at BOL in sphere-pac pins: the cladding tube is fully filled with particles. The heat transfer from the fuel surface to the clad is therefore enhanced in sphere-pac pins at BOL. With both fuels, the radial cladding temperature profile at core midplane is rather flat and

stabilizes after 50s at around 775K. The safety limits are therefore met. The fuel surface temperature is globally higher –by 45K– in the pellet than in the sphere-pac fuel, except for the hottest SIMMER ring where a gap closure in the pellet fuel occurs because of its high power. The fuel average temperature reaches a maximum difference of 831K between sphere-pac and pellet fuel in the hottest channel, leaving a margin to melting of 240K in case of the sphere-pac pin, see Fig. 5. Even though the fuel average temperature stays below its melting point, the center temperature of sphere-pac fuel pins – assessed by using bulk and surface node temperatures - exceeds the melting point in at least 3 rings and leads to fuel melting at steady state. This is due to the non-optimized WH BOL power profile. Additionally, nominal power was assumed for BOL: decreasing this power might prevent pin failures.

Attention is brought to the hottest ring. There, the cladding temperature already reaches 836K and 856K in case of pellet and sphere-pac pins, respectively. It has to be noticed that the cladding temperature in the pellet-core already exceeds the 823K limit for nominal conditions. The axial fuel surface temperature profile is depicted Fig. 6(a). It has to be stressed, that the pellet fuel axial temperature distribution reflects the large thermal expansion of the pellet especially at core midplane. As the core is at nominal power, fuel-cladding contact is made over the central part of the pin and the enhanced gap conductance leads to a dip in the fuel surface temperature in this area. On the bottom and top of the fuel column, the fuel surface temperature of the sphere-pac pin is significantly lower than the one in the pellet pin. This can be acknowledged to the missing gap in sphere-pac fuels enhancing the heat transfer from fuel to coolant. In the middle part, the hottest part of the pin, the tendency is reversed. Indeed, in this region, the pellet pin experiences gap closure. As the thermal conductivity of pellet fuel is higher than the sphere-pac fuel one, the heat transfer is enhanced and the fuel temperature is decreased. As concerns the fuel bulk temperature, the sphere-pac pin presents considerably higher temperatures than the pellet pin, Fig. 6(b).

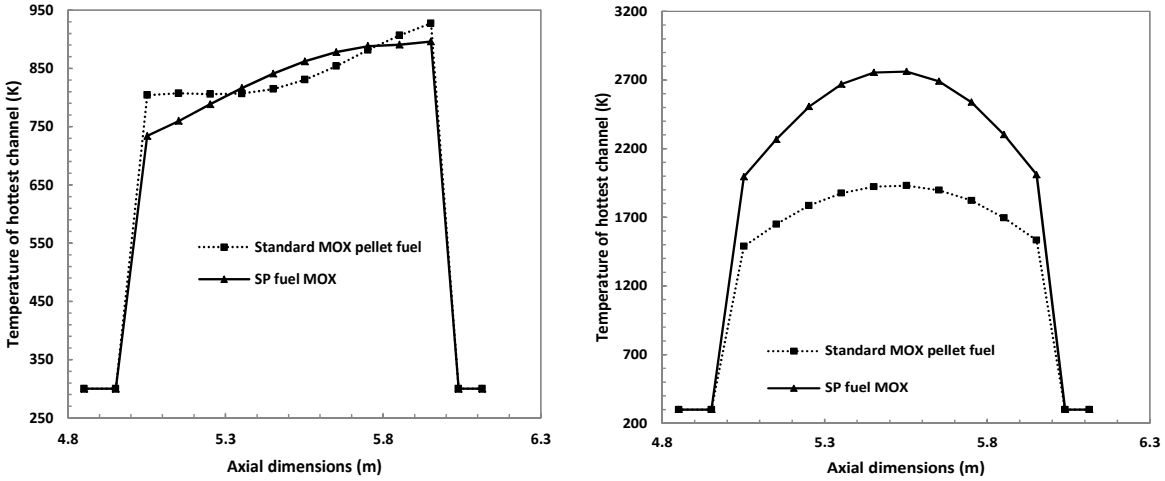

Fig. 6. BOL axial fuel temperature distribution in the WH hottest channel in case of a sphere-pac and pellet pin.

(a) surface temperature; (b) bulk temperature.

- End of equilibrium cycle calculations

At EOEC, because of the similar thermal conductivities of sphere-pac and pellet fuel, no significant difference is observed. The maximum fuel bulk temperature reaches 1620K and stays appreciably below the melting temperature of 3002K. In addition the WH radial power profile and related gagging scheme are optimized.

It was shown that the WH could be loaded with sphere-pac instead of pellet fuels assuming pins with a smear density as high as 83.41% can be fabricated. If the required fuel mass in the core cannot be reached, the fuel enrichment should be increased to obtain criticality, therefore worsening the thermal conductivity of the sphere-pac pins and impacting the core design. It has also to be stressed that restructuring of sphere-pac fuel happens very early, during the reactor start-up phase, producing a fuel with properties similar to pellet fuel. Consequently, as the macrostructure of irradiated sphere-pac fuels is close to the one of pellet fuels, calculations for irradiated sphere-pac fuels provide similar results to those obtained earlier in the CP-ESFR project [2].

4.2. ULOF calculations

A ULOF simulation is performed to get a first insight into the transient behavior of a sphere-pac fuel loaded core and to investigate model development needs for this innovative fuel. The ULOF simulation is started from steady state, requiring the simulation of effects like axial fuel and clad expansion. Analyses showed that the standard expansion models are not sufficient as in sphere-pac pins no pellet stack or gap do exist. A model development to improve the representation of sphere-pac fuels under transient conditions has therefore been started. The need for experimental support is evident. For the current calculation the transient is simulated taking into account the Doppler feedback only, its main purpose being the identification of modeling needs. Starting from steady state, the pump coast down is initiated with a flow halving time of 10s following the law:

$$\Delta p = \Delta p_0 \frac{1}{(1+\frac{t}{10})} \tag{4}$$

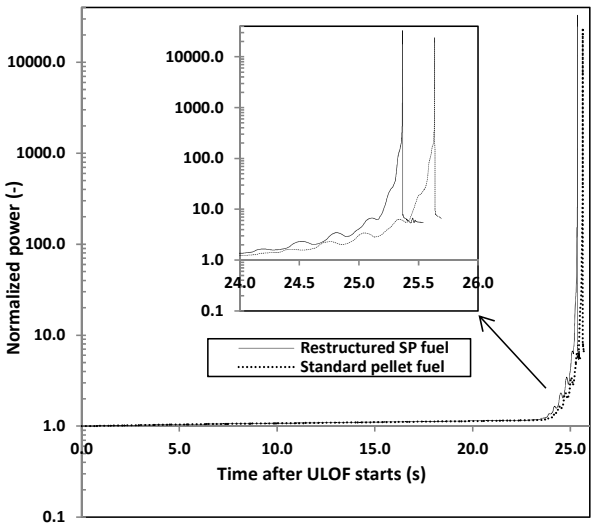

Fig. 7. Power evolution during ULOF.

Due to the lack of coolant circulation, heat is not sufficiently evacuated from the fuel pins and the coolant temperature rises. The reactivity increases smoothly, as the rise in fuel temperature makes the Doppler effect counterbalance the sodium density effect. In case of the pellet fuel loaded core, sodium boiling starts at 21.5s in the 13th channel. It is followed 2.8s later by channel 9 and 10, and quickly after by channels 7, 11, 3 and 6. During this voiding propagation, the reactivity is oscillating. 4.13s after boiling onset all fuel channels except the outermost one

experience voiding. At this time, reactivity reaches 1$ in the calculation putting the reactor in a prompt supercritical state and triggering the first power peak. Simultaneously, fuel melting occurs in channel 13, leading to pin disruption. Around 25.63s, overall fuel melting has occurred. Due to fuel and cladding dispersion, the power rapidly decreases. It can be observed that under the previously described simulation conditions the accident evolution is similar for both fuel types. Both first power peak values (Fig. 7) and consequently both thermal energy releases are close, leading to the conclusion that the accident behavior is independent of the fuel type in the current simulation.

Modeling efforts are under way to include the mitigating core expansion feedbacks. As SIMMER-III has a space-time dependent neutronic model with permanent cross-sections updating, solved on an Eulerian grid, it was decided to head for a more general solution of the expansion problem than simulating expansion effects with reactivity coefficients. Different methods are currently investigated at KIT to take into account the axial and radial expansion feedbacks from fuel, clad and structure: instead of expanding the mesh, reflecting a Lagrangian approach, the mesh is kept equal to the original one while the cross sections are adequately modified.

5. Conclusions

A preliminary safety assessment of the WH loaded either with (U,Pu) mixed oxide sphere-pac or pellet fuel was performed. Emphasis was put on a peculiar thermo-physical parameter for sphere-pac fuel: the thermal conductivity. In the first step the feasibility of using sphere-pac fuel into a standard SFR core could be proven. Analyses showed that a BOL core with this fuel would undergo fuel melting in at least three channels, assuming no restructuring took place in the fuel. However one has to note that the results do reflect the first hours of the core, assuming full power operation in the WH BOL core with high radial power peaking factors. For a core with restructured fuel which is the case of fuel subjected to 3 irradiation cycles, the fuel type doesn't impact anymore the fuel temperature distribution. A ULOF accident is expected to proceed in an analogous way for both fuel types. Future work is intended to cope with the core thermal expansion effects as they might considerably impact the results and a more distinct behavior might be observed in case of sphere-pac fuels.

Acknowledgements

The authors appreciate the efforts and support of all scientists and institutions involved in the FP-7 PELGRIMM Project, as well as the financial support of the European Commission through the grant agreement 295664.

References

[1] F. Delage et al. , Investigation of Pelletized and Sphere-Packed Oxide Fuels for Minor Actinide Transmutation in Sodium Fast Reactors, Within the FP-7 European Project Pelgrimm, IEMPT-12, 2012, Prague, Czech Republic.
[2] G. L. Fiorini et al. , The collaborative project on European sodium fast reactor (CP-ESFR project), Conference FISA 2009, Prague, Czech Republic.
[3] B. Vezzoni, et al, Optimization of Safety Parameters and Accident Mitigation Measures for Innovative Fast Reactor Concepts, ICENES, May 15 - 19, 2011, San Francisco, USA
[4] B. Vezzoni, et al. Safety-Related Optimization and Analyses of an Innovative Fast Reactor Concept, Journal Sustainability, June 2012, Vol. 4, pp. 1274-1291.
[5] Sa. Kondo et al., "SIMMER-III: A Computer Program for LMFR Core Disruptive Accident Analysis, Version 2.H Model Summary and Program Description," JNC TN9400 2001-002
[6] M. A. Pouchon et al., Sphere-pac and Vipac fuel, in: R. J. M. Konings, Comprehensive nuclear materials, Elsevier, 2012, pp. 275–312.
[7] R. K. McGeary, Mechanical packing of spherical particles, Journal of The American Ceramic Society, Vol. 44, No. 10, 1961, pp. 513-522.
[8] K. Morita et al, SIMMER-III Analytic Thermo physical Property Model, 1999, O-arai engineering Center, Japan Nuclear Cycle Development Institute, JNC TN9400 2000-004.
[9] R.O.A Hall et al. , The thermal conductivity of powder beds. A model, some measurements on UO2 vibro-compacted microspheres, and their correlation, Journal of Nuclear Materials 101, 1981, pp 172-183.
[10] http://www.cp-esfr.eu/index.php
[11] Y. Philipponneau, Thermal conductivity of (U,Pu)O2-x mixed oxide fuel, Journal of Nuclear Materials 188, 1992, pp 194-197.

[12]K. Kamiyama et al. , SIMMER-III Structure Model – Model and Method Description, 2004, O-arai engineering Center, Japan Nuclear Cycle Development Institute, JNC TN9400 2004-043.